Intraoperative Immunophotodetection for Radical Resection of Cancers: Evaluation in an Experimental Model[1]

Marian Gutowski,[2] Magali Carcenac,[2] Didier Pourquier, Christian Larroque, Bernard Saint-Aubert, Philippe Rouanet, and André Pèlegrin[3]

Department of Oncologic and Reconstructive Surgery [M. G., B. S-A., P. R.], JE2176 Université Montpellier I, Cancer Research Center [M. C., A. P.], and Department of Pathology [D. P.], Cancer Institute Val d'Aurelle—Paul Lamarque, Montpellier, Cedex 5, France, and INSERM U128, Montpellier 34000, France [C. L.]

ABSTRACT

The aim of our study was to assess the technique of immunophotodetection (IPD) in intraoperative situations in an experimental model and to determine its capacity to detect very small tumor masses. IPD is a recent technology involving fluorescent dye-labeled monoclonal antibodies (MAbs) directed against tumor-associated antigens. Up to now, no intraoperative device for IPD has been developed, and limits of detection of the technique are unknown. MAb-dye conjugates were prepared using the anti-carcinoembryonic antigen MAb 35A7 labeled with indocyanine and ^{125}I. Time-dependent (6, 12, 24, 48, and 96 h post i.v. injection) and dose-dependent (10, 40, and 100 μg of conjugate) biodistribution studies were performed in nude mice bearing an LS174T peritoneal carcinomatosis demonstrating high tumor uptake (up to 21% of the injected dose/g of tumor 48 h postinjection). Intraoperative IPD was studied, using a newly developed device, in 16 mice 48 h after i.v. injection of 40 μg of the ^{125}I-MAb 35A7-indocyanine conjugate. The fluorescent status of 333 biopsies was compared with their histological analysis. Sensitivity was 90.7%, specificity was 97.2%, the positive predictive value was 94.7%, and the negative predictive value was 94.9%. Detection of very small nodules (<1 mg in weight or <1 mm in diameter) was possible. However, we observed a decrease in sensitivity as a function of tumor mass: 100% for nodules >10 mg *versus* 78% for nodules ≤1 mg. These experiments demonstrate that intraoperative IPD is easy to use and associated with high sensitivity and specificity, even for low tumor masses. On the basis of these encouraging results, intraoperative IPD should be assessed in a clinical study.

INTRODUCTION

Cancers are characterized by their ability to produce local or metastatic recurrences. Despite major progress in diagnostic techniques and treatments, prognosis is often associated with radical first surgery. One way to improve surgical performance is to provide the surgeon with intraoperative detection and diagnostic methods for cancer eradication.

Photodetection was developed in the 1980s with the use of hematoporphyrin derivates such as Photofrin (1, 2). The major limitations of photodiagnosis with these molecules are their low selectivity for cancerous tissues and their capacity to react chemically and induce high photosensitization or necrosis. This latter limitation is, in fact, an advantage in photodynamic therapy.

IPD[4] is a more recent technology using MAbs labeled with a dye. Given the tumor- seeking capacities of MAbs directed against tumor-associated antigens such as CEA, they can be used as vehicles to concentrate dyes in tumors. Dyes are chosen on the basis of their spectral and photochemical properties. IPD feasibility was first demonstrated in experimental and clinical research with fluorescein-labeled MAbs (1–3). However, because of its low excitation and emission wavelengths, fluorescein has two major drawbacks: (*a*) a low tissue penetration; and (*b*) nonspecific autofluorescence of the normal tissues induced by the exciting laser light. These problems have been overcome with the use of indocyanine, a dye with longer excitation and emission wavelengths, allowing higher tissue penetration, and avoiding nonspecific autofluorescence (4).

With MAb-indocyanine conjugates, IPD appears more attractive, in particular, in intraoperative situations where the surgeons are interested in a so-called optical biopsy approach to guide them in their search for tumor tissue. This concept is based on the possibility of acquiring histological information by direct or indirect visualization. However, no material has been developed yet for intraoperative IPD, and the detection threshold is unknown. The purpose of the present study was to evaluate the capacity of tumor detection with a specially designed material for the detection of the smallest possible tumor mass.

Received 12/8/00; revised 2/2/01; accepted 2/5/01.
The costs of publication of this article were defrayed in part by the payment of page charges. This article must therefore be hereby marked *advertisement* in accordance with 18 U.S.C. Section 1734 solely to indicate this fact.
[1] This work was supported by the Institut National de la Santé et de la Recherche Médicale (contrat ERCA), the Ligue Nationale Contre le Cancer (Comité de l'Hérault et Conseil Scientifique National), and the Caisse d'Assurances Maladie des Professions Libérales Province.
[2] Marian Gutowski and Magali Carcenac are to be considered as equal coauthors.
[3] To whom requests for reprints should be addressed, at Centre de Recherche en Cancérologie, Centre Régional de Lutte contre le Cancer Val d'Aurelle—Paul Lamarque, Parc Euromédecine, 34298 Montpellier, Cedex 5, France. Telephone: 33-4-67-61-30-32; Fax: 33-4-67-61-37-87; E-mail: apelegrin@valdorel.fnclcc.fr.

[4] The abbreviations used are: IPD, immunophotodetection; MAb, monoclonal antibody; CEA, carcinoembryonic antigen; % ID/g, percentage of injected dose/gram; RAID, radioimmunodetection; RIGS, radioimmunoguided surgery; HpD, hematoporphyrin derivatives.

MATERIALS AND METHODS

Nude Mice Tumor Model. The CEA-expressing human colon carcinoma LS174T cell line (5) was purchased from the American Type Culture Collection (Rockville, MD). A peritoneal carcinomatosis was induced by i.p. injection of 2×10^6 cells in 200 μl serum-free culture medium into Swiss nude mice (Iffa Credo, L'Arbresle, France). All of the experiments were performed in compliance with the French guidelines for experimental animal studies (Agreement No. 5542).

MAbs and Radiolabeling Procedures. Antibodies were purified from mouse ascites using ammonium sulfate (45% saturation at 4°C) precipitation and then DE52 cellulose (Whatman, Balston, United Kingdom) ion-exchange chromatography using 0.03 M/liter or 0.05 M/liter phosphate buffer (pH 8).

MAb 35A7 is an IgG1 specific for the CEA GOLD 2 epitope and does not bind to cross-reacting antigens or to granulocytes (6, 7). This MAb has already been used in therapeutic and radiodiagnostic studies (8, 9). In control experiments, MAb P3X63 purified from secreting mouse myeloma was used as irrelevant IgG1 (10).

Batches of 1–2 mg of MAb 35A7 or P3X63 were labeled with 300–500 μCi ^{125}I or ^{131}I (1Ci = 37 GBq) by iodogen (Pierce, Rockford, IL) method. Free ^{125}I or ^{131}I was separated from labeled MAb on a Sephadex-G25 column (Amersham Pharmacia Biotech AB, Uppsala, Sweden) equilibrated in 0.1 M sodium bicarbonate buffer (pH 9.3).

Preparation of Indocyanine—MAb Conjugates. Indocyanine (Cy5; Amersham Life Science, Arlington Heights, IL) was diluted in pure dimethylformamide (100 μl per dye vial). Twenty-five μl of this solution were added dropwise to 1 mg of ^{125}I-MAb (at a concentration of 1 mg/ml) in a glass tube. After 4 h at room temperature and in the dark, the conjugate was filtered through a Sephadex-G25 column equilibrated in PBS (pH 7.4) to remove free dye. The indocyanine:MAb molar ratio was determined by using the absorbance at 649 nm for the indocyanine concentration and the radioactivity for the MAb quantitation.

The immunoreactivity of the conjugates was determined *in vitro* by a direct binding assay. Twenty ng of conjugate were incubated for 16 h at 37°C with 3 μg of purified CEA chemically coupled to Sepharose-CNBR (Pharmacia) in PBS containing 0.1% BSA and 1% normal mouse serum. The percentage of binding was determined by measuring the radioactivity bound to CEA. The nonspecific binding was determined with MAb P3X63 as irrelevant protein coupled to Sepharose.

The presence of aggregated material eventually generated by the labeling process was determined by filtration of a conjugate sample through a Sephacryl S200 gel column (Pharmacia).

***In vitro* Stability of the Conjugates.** To test the stability, 1 mg of ^{125}I-MAb 35A7-$(Cy5)_3$ was incubated for 48 h at 37°C with 600 μl of normal mouse serum containing 0.1% sodium azide. After separation by gel filtration on a Sephacryl S200 column (Pharmacia), the absorbance of the eluent at 280 and 649 nm and the ^{125}I radioactivity were measured.

***In Vivo* Tumor Localization of Radiolabeled Conjugates.** Ten μg of ^{125}I-MAb 35A7-$(Cy5)_2$ conjugate mixed with 10 μg ^{131}I-MAb P3X63-$(Cy5)_2$ were injected i.v. into nude mice bearing an LS174T peritoneal carcinomatosis. Mice had their thyroid blocked by adding Lugol's (0.05%) iodine solution in the drinking water. To determine the kinetics of tumor localization and the biodistribution of the conjugate, groups of five mice were killed and dissected at different time intervals: 6, 12, 24, 48, and 96 h after injection. The tumor and all normal organs, including a 0.5-ml blood sample, were weighed and their ^{125}I and ^{131}I radioactivities were measured in a dual channel scintillation counter. Iodine radioactivity measurement in the tissues correlates with the MAb-dye conjugate concentration because, after catabolism, free iodine is not kept within the cells and is eliminated rapidly (11). Results were expressed as % ID/g of tissue. The tumor:normal tissue ratios were calculated by dividing the % ID/g in the tumor by that measured in each individual organ.

Intraoperative IPD. IPD was performed using a device specially designed by BFP Electronique (Marvejols, France) for intraoperative use. Excitation was provided by a cooled laser diode emitting light at 649 nm through a fiber-optic output. Intraoperative detection was imaged using a high definition black and white CCD camera system (CV-M1; JAI Corporation, Kanagawa, Japan) equipped with an interference filter (NR JVC 83/6; Melles Griot). The camera was connected to a computer, and images were acquired using Optimas software (Media-Cybernetics, Silver Spring, MD).

Mice received *i.v.* injections of 10, 40, or 100 μg of the ^{125}I-MAb 35A7-$(Cy5)_3$ conjugate corresponding to 0.15–1.5 μg of indocyanine. Animals were killed 48 h after injection and fluorescence was analyzed. Fluorescent nodules <3 mm in diameter were dissected, measured, and weighed. As described above, biodistribution of the conjugate in the tissues and the fluorescent nodules in each mouse was determined. Systematic biopsies were performed on the diaphragm, omentum, mesentery, mesocolon, and Douglas' pouch. A group of five control animals received 40 μg ^{125}I-MAb P3X63-$(Cy5)_3$ and IPD was performed in the same way. The biodistribution results were expressed as % ID/g of tissue.

Histological Analysis. All biopsies and dissected tissues were histologically analyzed after H&E staining. When needed, immunohistological analysis was performed, using the anti-CEA chimeric mouse-human MAb X4 (12) as primary antibody (10 μg/ml for 30 mn), followed by incubation for 30 min with horseradish peroxidase-conjugated antihuman IgG (Dako P214; dilution, 1:50). The staining reaction was performed using AEC as substrate and slides were counterstained with hematoxylin.

Performance Parameters and Statistical Analysis. The histological results were compared with the fluorescence data and reported in contingency tables. Sensitivity, specificity, and positive and negative predictive values were then calculated. Confidence limits were calculated from the binomial distribution.

RESULTS

***In Vitro* Characterization and Stability of Indocyanine—MAb Conjugates.** Indocyanine was solubilized in pure dimethylformamide and incubated at room temperature for 4 h with MAb 35A7 previously labeled with trace amounts of ^{125}I. The conjugate preparations gave a single protein peak after

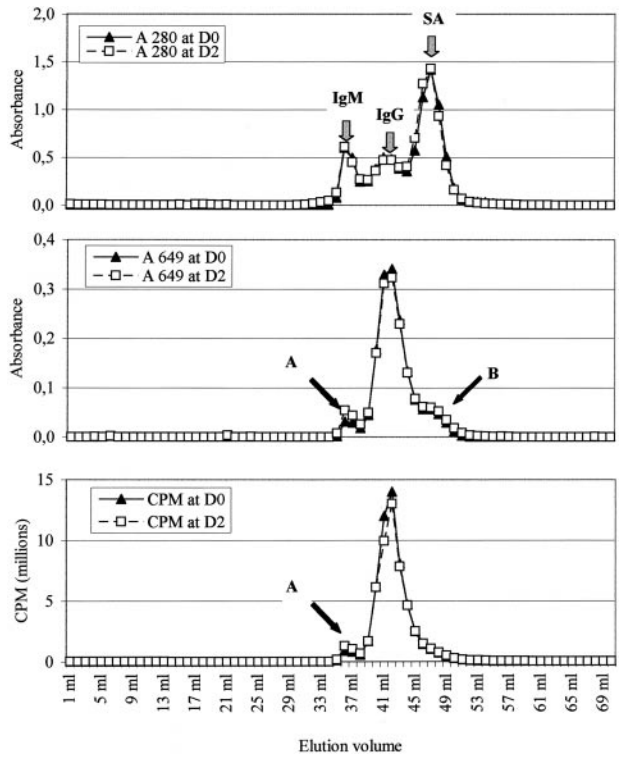

Fig. 1 Elution profile on Sephacryl S200 column of the ^{125}I-MAb 35A7-$(Cy5)_3$ conjugate after incubation in normal mouse serum for 48 h at 37°C, demonstrating the *in vitro* stability of the conjugate. The three diagrams show absorbances (*A*) at 280 nm (proteins) and 649 nm (indocyanine) and ^{125}I radioactivity. The *grey arrows* indicate the peaks of mouse IgM, IgG, and serum albumin. *A*, aggregates; *B*, a fraction of free dye bound to serum albumin. *D0* and *D2*: day 0 and day 2.

filtration on Sephacryl S200 with <3% of aggregates. The MAb 35A7 to indocyanine molar ratio ranged from 2 to 3. The percentage of binding of the ^{125}I-MAb 35A7-$(Cy5)_{2-3}$ conjugate to insolubilized CEA was at least 80%. Binding to control (MAb P3X63) was <3%.

The stability of the ^{125}I-MAb 35A7-$(Cy5)_3$ conjugate was studied *in vitro* after incubation for 48 h at 37°C in normal mouse serum (Fig. 1). Subsequent filtration of the conjugate on Sephacryl S200 showed that absorption at 649 nm strongly correlated with the radioactivity. The two labels, ^{125}I and indocyanine, were stable under these conditions. A first peak at 649 nm (labeled "*A* " in Fig. 1), representing 5–10% of the conjugate, suggested the presence of aggregates. However, these aggregates were not formed entirely during the incubation period. Another small peak (labeled "*B* " in Fig. 1) suggested the fixation of free dye on serum albumin.

***In Vivo* Tumor Localization and Biodistribution of ^{125}I-MAb 35A7-$(Cy5)_3$ Conjugates.** Five groups of five mice bearing an LS174T peritoneal carcinomatosis were given i.v. injections of 10 μg ^{125}I-MAb 35A7-$(Cy5)_3$ conjugate and 10 μg ^{131}I-MAb P3X63-$(Cy5)_3$ conjugate as negative control. Injections were performed 6, 12, 24, 48, or 96 h before killing. For the biodistribution analysis, all of the carcinomatosis nodules were pooled to obtain a unique value. As shown in Fig. 2, the % ID/g of tumor was already 16.5 ± 4.9% at 24 h postinjection, reached 21.0 ± 7.8% at 48 h, and decreased to 8.5 ± 4.5% at 96 h. In contrast, the % ID/g of normal tissue decreased regularly with a value of 11.1 ± 1%, 7.1 ± 1.6%, and 1.2 ± 1.2% at 24, 48, and 96 h, respectively, for blood. The highest tumor: normal tissue ratios were observed at 48 h. They ranged from 2.9 ± 0.3 for the blood to 59.5 ± 6.3 for the colon, with representative values of 8.9 ± 1, 14.7 ± 1.4, 6.7 ± 0.7, 26.5 ± 2.6, and 30.5 ± 3.4 for the liver, kidneys, lungs, muscle, and small bowel, respectively. The ratios of % ID/g tumor:% ID/g of the entire mouse except the tumor ranged from 1.8 ± 0.6 at 6 h to 10.2 ± 4.5 at 48 h and finally decreased to 1.8 ± 0.4 at 96 h.

These biodistribution experiments were performed because all of our previous IPD and immunophototherapy studies had been done with s.c. T380 human colon carcinoma tumors (1, 13). According to the results of the present kinetic studies (Fig. 2), we decided to perform IPD 48 h postinjection. As shown in Fig. 2, the irrelevant conjugate ^{131}I-P3X63-$(Cy5)_3$ had no selective localization in the human colon carcinoma xenograft.

Intraoperative IPD of an LS174T Peritoneal Carcinomatosis in Nude Mice. Groups of five mice bearing an LS174T peritoneal carcinomatosis were given i.v. injections of the ^{125}I-MAb 35A7-$(Cy5)_3$ conjugate 48 h before killing. Intraoperative IPD was performed in three steps: frame acquisition before laparotomy, after laparotomy, and after dissection of the smallest tumor nodules (Fig. 3). After IPD, each mouse was entirely dissected, and the biodistribution of the conjugate was analyzed.

To determine the lowest dose of conjugate permitting IPD, three groups of mice received different doses of the ^{125}I-MAb 35A7-$(Cy5)_3$ conjugate: 10, 40, and 100 μg. Whatever the dose of the conjugate injected, all superficial tumor nodules were detected, but with difficulties for the group that received the 10-μg dose of conjugate corresponding to about 0.15 μg of indocyanine. The fluorescence signal in the latter group was clearly weaker than in the other groups. It was only perceptible upon strong excitation (>30 mW/cm^2) responsible for a decrease of the signal-to-noise ratio. Performance parameters are given in Table 1.

The ^{125}I-MAb 35A7-$(Cy5)_3$ conjugate tumor uptake was not dose-dependent, giving 21.1 ± 6.3, 22.6 ± 4.1, and 21.6 ± 3.3% ID/g for mice injected with 10, 40, and 100 μg of conjugate, respectively. Consequently, absolute quantities of injected indocyanine localized in the tumor ranged from 30 to 300 ng/g, which explains the differences in laser-induced fluorescence. We also observed a decrease of the tumor:normal tissue ratios with increasing doses of conjugate. For representative organs such as liver and kidneys, these ratios were 11.7, 8.1, and 8.3 and 19.2, 16.1, and 12 for mice injected with 10, 40 or 100 μg dose of conjugate, respectively.

On the basis of these results, 16 mice bearing an LS174T peritoneal carcinomatosis were given 40 μg of the ^{125}I-MAb 35A7-$(Cy5)_3$ conjugate 48 h before killing and intraoperative IPD. Biopsies were performed on all of the fluorescent nodules and systematically on the diaphragm, mesocolon, mesentery, omentum, and Douglas' pouch. The fluorescence status of each of these 333 biopsies was compared with histological analysis to determine the sensitivity, specificity, and positive and negative predictive values (Table 2).

All fluorescent nodules were divided in three groups ac-

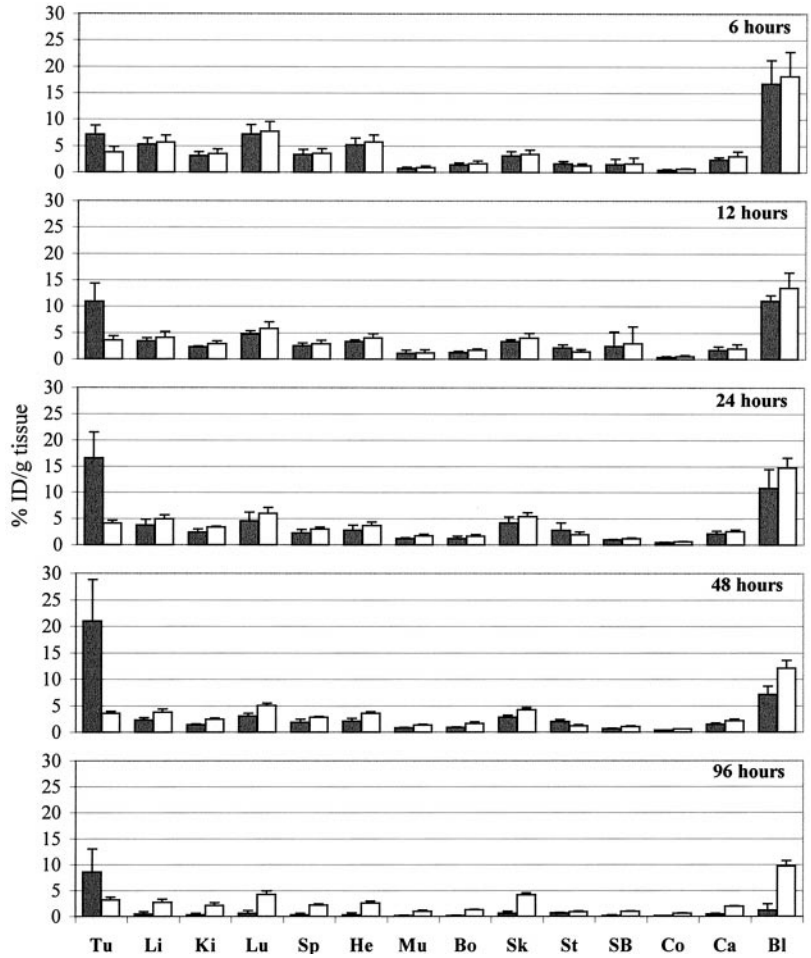

Fig. 2 Time-dependent study of the biodistribution of the ^{125} I-MAb 35A7-$(Cy5)_3$ conjugate in nude mice bearing an LS174T peritoneal carcinomatosis. Ten μg of conjugate were injected i.v. 6, 12, 24, 48, or 96 h before killing. Mice were also given i.v. 10 μg of the irrelevant conjugate ^{131}I-MAb P3X63-$(Cy5)_3$ as control. The % ID/g of tissue was determined by measurement of radioactivity. *Tu*, tumor; *Li*, liver; *Ki*, kidneys; *Lu*, lungs; *Sp*, spleen; *He*, heart; *Mu*, muscle; *Bo*, bone; *Sk*, skin; *St*, stomach; *SB*, small bowel; *Co*, colon; *Ca*, carcass; *Bl*, blood. ▨, ^{125}I-MAb35A7-$(Cy5)_3$; □, ^{131}I-MAb P3X63-$(Cy5)_3$.

cording to their masses (≤1 mg, >1, and ≤10 mg, or >10 mg) to analyze the importance of the mass on the sensitivity of the IPD (Table 3). The tumor nature was confirmed for all of the fluorescent nodules larger than 10 mg (100% sensitivity). For nodules smaller than 1 mg, the IPD sensitivity was still as high as 78%. In these nodules, the amount of conjugate was <100 ng, corresponding to ~1 ng of indocyanine. Dimensions of tumor nodules smaller than 1 mg were <1 millimeter, and five of these nodules were completely undetectable with the naked eye or by touch.

After IPD, each mouse was entirely dissected, and the biodistribution of the conjugate was analyzed. The ^{125}I-MAb 35A7-$(Cy5)_3$ conjugate uptake in the pooled nodules was found to be 23.1 ± 1.4% ID/g tumor.

As a negative control, five mice bearing LS174T peritoneal carcinomatoses were given 40-μg i.v. injections of ^{125}I-MAb P3X63-$(Cy5)_2$ conjugate 48 h before killing. During intraoperative IPD, we observed eight weakly fluorescent tumor nodules, each of which was >1 mg. These nodules were found in the presence of other tumor nodules which were not fluorescent.

DISCUSSION

The natural history of cancers is to produce local or metastatic recurrences, which often result in death of the patients. For many cancers, prognosis is bound to a maximal cytoreduction or, better, to radical resection. The idea of radical resection has led surgeons to aggressive surgery such as debulking procedures, used, for example, in peritoneal carcinomatosis induced by ovarian or colorectal cancers. One problem confronting the surgeon is to identify tumor tissues. This difficulty can result in incomplete removal of the tumor mass or systematic extensive surgery (like node curage), which is sometimes the source of postoperative complications. One way to avoid these problems is to provide the surgeon with the possibility of distinguishing tumor tissues from benign ones. Cancer detection or imaging has been developed in the past 20 years, and two technologies in particular have been studied: RAID and photodetection.

RAID permitted the first detection and localization of a cancer by external radiophotoscanning after injection of a radiolabeled anti-CEA IgG (14, 15). This technology uses radiolabeled MAbs against different molecular targets, especially tumor-associated antigens such as CEA. Because of its high CEA expression, colorectal carcinoma has often been studied in human xenografts and clinical trials. The sensitivity and specificity of such conjugates ranges from 80 to 90% with radioiodine labels of MAb, and tumor resolution can reach 1.5–2 cm (16). RAID is used for external scanning and imaging, and no real-time and intraoperative imaging procedure has been devel-

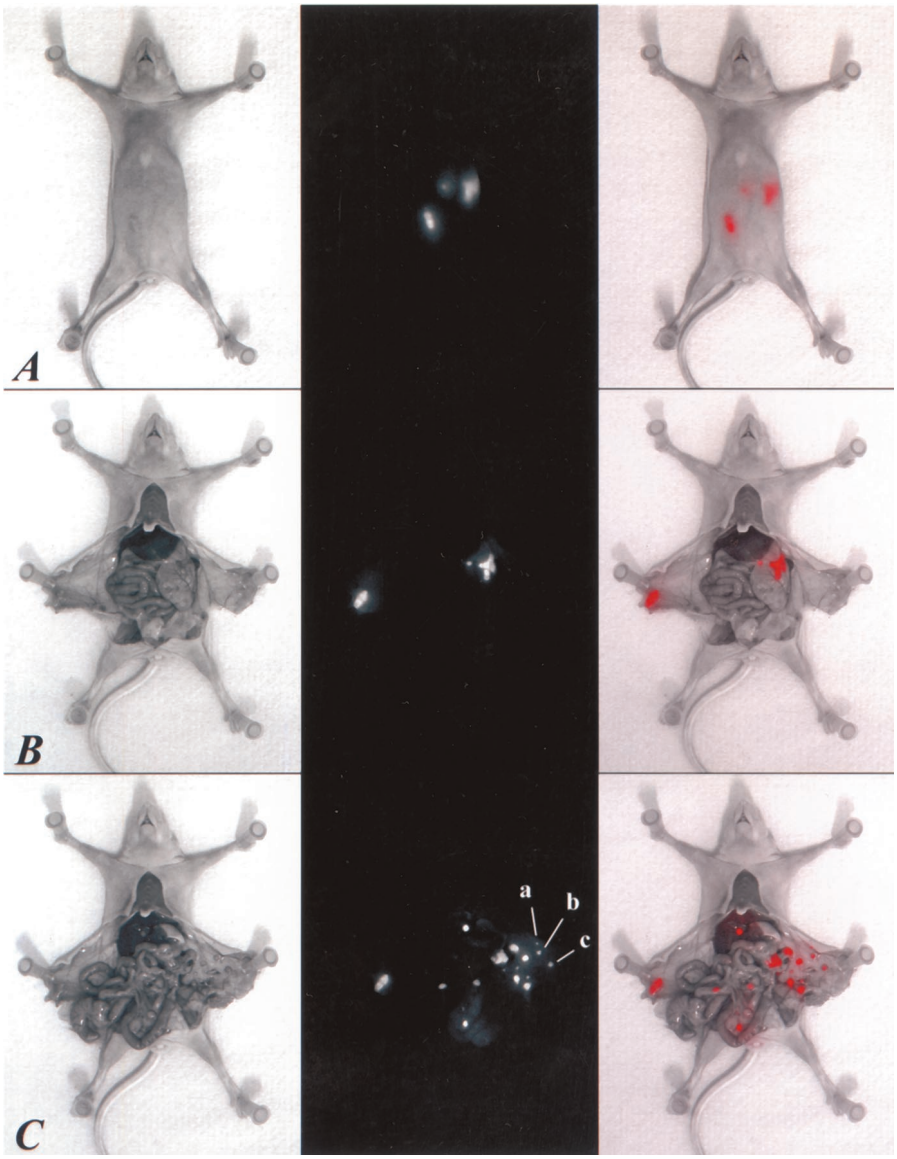

Fig. 3 Intraoperative IPD of peritoneal carcinomatosis in a nude mouse. The mouse received 40 μg of the ^{125}I-MAb 35A7-$(Cy5)_3$ conjugate 48 h before killing. Images are subdivided in three, from *left to right*: image before excitation; filtered image after excitation; and digital combination of the images. *A*, observation before laparotomy. Some tumor nodules are already visible: the xenograft injection point and intra-abdominal nodules. *B*, observation after laparotomy. Good correlation with nodules seen in *A*. *C*, observation after dissection of the smallest nodules. Nodules *a*, *b*, and *c* weighed <1 mg and contained between 1 and 2 ng of indocyanine.

oped, whereas the RIGS technique permits intraoperative detection of cancers using radiolabeled antibodies and γ probes (17).

Photodetection was built on the use of dyes, HpD, selected for their dual capacity to accumulate in tumor and to produce laser-induced fluorescence. Since the 1980s, investigators have been studying the feasibility and performance of photodetection with HpD, and clinical feasibility was even demonstrated by endoscopic diagnosis of tumors (18, 19). Despite major progress in signal treatment, no intraoperative device has been developed to permit real-time imaging and diagnosis. Furthermore, there are several limiting factors associated with the use of HpD and their purified derivative, Photofrin II. These products have a poor capacity to accumulate in tumor tissues, their fluorescence quantum yield is low, and they induce a photochemical reaction with the production of singlet oxygen. This chemical effect, responsible for photosensitization, was later used for photodynamic therapy trials but has proven to be a drawback in cancer detection (20).

IPD has been developed to combine the advantages of RAID and photodetection. MAbs directed against tumor-associated antigens have been used as vectors for tumor localization and have been labeled with dyes selected for their spectral and photochemical properties. Criteria for dye selection are: (*a*) high excitation and emission wavelengths for deep penetration in tissues; (*b*) high molar extinction coefficient; (*c*) high fluorescence quantum yield; and (*d*) low singlet oxygen quantum yield. In our study, we selected indocyanine for the following reasons: (*a*) far-red excitation and emission wavelengths, 649 and 670 nm, respectively; (*b*) fluorescence quantum yield >0.28 (for a molecular dye:MAb ratio of 2); (*c*) a high molar extinction coefficient ($E^{IM}_{lcm} = 2.5 \times 10^5$); (*d*) a very low quantum yield of singlet oxygen; and (*e*) high solubility in water. Experimental

Table 1 Comparison of intraoperative IPD performance as a function of the dose of the ^{125}I-MAb 35A7-(Cy5)$_3$ conjugate injected

	Amount of ^{125}I-35A7-(Cy5)$_3$ conjugate injected		
	10 μg	40 μg	100 μg
Sensitivity	97.8% (88.5–99.9%)[a]	86.0% (71.4–93.0%)	83.6% (71.2–92.2%)
Specificity	98.6% (92.5–99.9%)	98.4% (91.5–99.9%)	100.0% (94.6–100.0%)
PPV[b]	97.8% (88.5–99.9%)	97.7% (88.0–99.9%)	100.0% (92.3–100.0%)
NPV[c]	98.6% (92.5–99.9%)	89.8% (80.2–95.8%)	88.0% (78.5–94.4%)

[a] Results are given in percentiles with 95% confidence limits in parentheses.
[b] PPV, positive predictive value.
[c] NPV, negative predictive value.

Table 2 Overall results of intraoperative immunophotodetection in nude mice bearing a LS174T peritoneal carcinomatosis

Biopsies were taken of fluorescent tissues and systematically of the diaphragm, mesocolon, mesentery, omentum, and Douglas pouch.

	Presence of tumor	
	Yes	No
Fluorescence		
Yes	108	6
No	11	208
		Confidence limits (95%)
Sensitivity	90.7%	86.8–93.2%
Specificity	97.2%	95.5–98.9%
PPV[a]	94.7%	92.3–97.0%
NPV[b]	94.9%	92.1–96.6%

[a] PPV, positive predictive value.
[b] NPV, negative predictive value.

Table 3 Results of biopsies on fluorescent tissues as a function of their mass

Biopsy mass	Presence of tumor		PPV[a]	Confidence limits (95%)
	Yes	No		
>10 mg	38	0	100%	90.8–100%
>1 mg and ≤10 mg	32	1	96.9%	84.2–99.9%
≤1 mg	38	5	88.4%	74.9–96.1%

[a] PPV, positive predictive value.

studies and clinical trials have already demonstrated the feasibility of IPD to detect tumor nodules (1, 2, 21, 22) as well as angiogenic markers (23), but never in an intraoperative situation. Our goal was to study the limits of IPD with a new device designed for intraoperative use.

The magnitude of fluorescence depends on three factors: the fluence rate distribution of excitation light, the product of the absorption coefficient and the quantum yield of the fluorophores, and the attenuation of the fluorescence light by absorption and scattering in tissues (24). Scattering also modifies the direction of light propagation, the fluorescence magnitude, and possibly the distribution of escape angles. False negatives found in this study corresponded to deep small tumor nodules which, after laser beam excitation, produced a weak fluorescent light, undetectable with our device because of scattering and absorption by tissues. On the basis of these data, we think that small and deep tumor nodules could be detected after technological progress in detection and signal treatment.

Using the anti-CEA-dye conjugate, we observed a few false positives in lymph nodes and biopsies with inflammatory infiltration. These results may suggest conjugate capture by inflammatory tissues and may be explained by the use of intact MAbs, which can be trapped by Fc receptor-positive inflammatory cells. We also observed a weak fluorescence of eight tumor nodules when we used the irrelevant MAb P3X63-(Cy5)$_2$ conjugate. During this experiment, the tumor nodules were fluorescent only under strong laser excitation, and tumor localization never exceeded 4.5% ID/g.

Despite a few false negatives and positives, the performance of the intraoperative IPD technique was encouraging with a sensitivity of 90.7% (CI $^{95\%}$, 86.8–93.2%), a specificity of 97.2% (CI $^{95\%}$, 95.5–98.9%), a positive predictive value of 94.7% (CI $^{95\%}$, 92.3–97%), and a negative predictive value of 94.9% (CI $^{95\%}$, 92.1–96.6%). We detected very small tumor nodules with a mass <1 mg and diameter <1 mm and even invisible by other means. In fact, true limits of the performances of intraoperative IPD were technical. It was technically very difficult to isolate nodules smaller than 1 mg, and these nodules were at the limit of detection for our balance and gamma counter.

Intraoperative IPD and RIGS are in fact complementary surgical techniques. Tumor masses inside the body can be detected by RIGS by the use of radioactive antibodies. However, small tumors have to be situated as close as possible to the probe to be detected. Under these conditions, RIGS is quite comparable with intraoperative IPD. The major advantage of IPD over RIGS is that it provides an image of the fluorescent tumor nodule within its nontumor tissue environment. The size of the tumor nodules detected by intraoperative IPD in our experimental model is very much lower than that of the nodules detected by external RAID (about 1 mm *versus* 1.5–2 cm; Ref. 16). This detection threshold has to be confirmed in a clinical trial, but the present results suggest a clear advantage of intraoperative IPD over external RAID to detect low tumor masses.

Finally, several conclusions can be drawn from this study: (*a*) intraoperative IPD is feasible under clinical conditions and is very easy to use; (*b*) the overall performances are very encouraging, and very low quantities of indocyanine (<1 ng) are sufficient to visualize tumor nodules; (*c*) as in all animal experiments, caution is required in transposing observations to the clinical situation, but the quantities of conjugate localized in tumor in our study are compatible with quantities detected in

clinical studies with a % ID/g of tumor between 1 to 30 $\times$ 10^{-3} for the injection of 5–10 mg of conjugate (25); (*d*) tumor nodules nonvisible to the naked eye have been detected using this technology; and (*e*) IPD should now be evaluated in clinical trials using humanized or human antibodies, which are now available and which would prevent the formation of human antimouse antibodies.

ACKNOWLEDGMENTS

The authors thank Régine Niementchinsky, Sabine Bousquié, Geneviève Heinz, and Céline Passet for excellent technical assistance; Michel Brissac for help in performing animal experiments; Michèle Radal for the immunohistochemistry experiments; Dr. Andrew Kramar and Sophie Gourgou for statistical analysis; and Dr. Sharon Lynn Salhi for editorial assistance.

REFERENCES

1. Pèlegrin, A., Folli, S., Buchegger, F., Mach, J. P., Wagnières, G., and van den Bergh, H. Antibody-fluorescein conjugates for photoimmunodiagnosis of human colon carcinoma in nude mice. Cancer (Phila.), *67:* 2529–2537, 1991.

2. Folli, S., Wagnières, G., Pèlegrin, A., Calmes, J-M., Braichotte, D., Buchegger, F., Chalandon, Y., Givel, J. C., Châtelain, A., van den Bergh, H., and Mach, J-P. Immunophotodiagnosis of colon carcinomas in patients injected with fluoresceinated chimeric antibodies against carcinoembryonic antigen. Proc. Natl. Acad. Sci. USA, *89:* 7973–7977, 1992.

3. Tatsuta, M., Lishi, H., Ichii, M., Baba, M., Yamamoto, R., Okuda, S., and Kikuchi, K. Diagnosis of gastric cancers with fluorescein-labeled monoclonal antibodies to carcinoembryonic antigen. Lasers Surg. Med., *9:* 422–426, 1989.

4. Mujumdar, R. B., Ernst, L. A., Mujumdar, S. R., and Waggoner, A. S. Cyanine dye labeling reagents containing isothiocyanate groups. Cytometry, *10:* 11–19, 1989.

5. Rutzky, L. P., Kaye, C. I., Siciliano, M. J., Chao, M., and Kahan, B. D. Longitudinal karyotype and genetic signature analysis of cultured human colon adenocarcinoma cell lines LS180 and LS174T, Cancer Res. *40:* 1443–1448, 1980.

6. Haskell, C. M., Buchegger, F., Schreyer, M., Carrel, S., and Mach, J-P. Monoclonal antibodies to carcinoembryonic antigen: ionic strength as a factor in the selection of antibodies for immunoscintigraphy. Cancer Res., *43:* 3857–3864, 1983.

7. Nap, M., Hammarstrom, M. L., Bormer, O., Hammarstrom, S., Wagener, C., Handt, S., Schreyer, M., Mach, J. P., Buchegger, F., von Kleist, S., *et al.* Specificity and affinity of monoclonal antibodies against carcinoembryonic antigen. Cancer Res., *52:* 2329–2339, 1992.

8. Buchegger, F., Pèlegrin, A., Delaloye, B., Bischof-Delaloye, A., and Mach, J-P. 131-I labeled F(ab′)2 fragments are more efficient and less toxic than intact anti-CEA antibodies in radioimmunotherapy of large human colon carcinoma grafted in nude mice. J. Nucl. Med., *31:* 1035–1044, 1990.

9. Delaloye, B., Bischof Delaloye, A., Buchegger, F., von Fliedner, V., Grob, J. P., Volant, J. C., Pettavel, J., and Mach, J. P. Detection of colorectal carcinoma by emission-computerized tomography after injection of 123I-labeled Fab or F(ab′)2 fragments from monoclonal anti-carcinoembryonic antigen antibodies. J. Clin. Investig., *77:* 301–311, 1986.

10. Kohler, G., and Milstein, C. Continuous cultures of fused cells secreting antibody of predefined specificity. Nature (Lond.), *256:* 495–497, 1975.

11. Kurth, M., Pelegrin, A., Rose, K., Offord, R. E., Pochon, S., Mach, J. P., and Buchegger, F. Site-specific conjugation of a radioiodinated phenethylamine derivative to a monoclonal antibody results in increased radioactivity localization in tumor. J. Med. Chem., *36:* 1255–1261, 1993.

12. Hardman, N., Gill, L. L., De Winter, R. F., Wagner, K., Hollis, M., Businger, F., Ammaturo, D., Buchegger, F., Mach, J. P., and Heusser, C. Generation of a recombinant mouse-human chimaeric monoclonal antibody directed against human carcinoembryonic antigen. Int. J. Cancer, *44:* 424–433, 1989.

13. Carcenac, M., Larroque, C., Langlois, R., Van Lier, J. E., Artus, J. C., and Pèlegrin, A. Preparation, phototoxicity and biodistribution studies of anti-CEA MAb-phthalocyanine conjugates. Photochem. Photobiol., *70:* 930–936, 1999.

14. Goldenberg, D. M., DeLand, F., Kim, E., Bennett, S., Primus, F. J., VanNagell, J. R., Estes, N., DeSimone, P., and Rayburn, P. Use of radiolabeled antibodies to carcinoembryonic antigen for the detection and localization of diverse cancers by external photoscanning. N. Engl. J. Med., *298:* 1384–1388, 1978.

15. Mach, J-P., Carrel, S., Forni, M., Ritschard, J., Donath, A., and Alberto, P. Tumor localization of radiolabeled antibodies against carcinoembryonic antigen in patients with carcinoma. N. Engl. J. Med., *303:* 5–10, 1980.

16. Goldenberg, D. M. Perspectives on oncologic imaging with radiolabeled antibodies. Cancer (Phila.), *80:* 2431–2435, 1997.

17. de Labriolle-Vaylet, C., Cattan, P., Sarfati, E., Wioland, M., Billotey, C., Brocheriou, C., Rouvier, E., de Roquancourt, A., Rostene, W., Askienazy, S., Barbet, J., Milhaud, G., and Gruaz-Guyon, A. Successful surgical removal of occult metastases of medullary thyroid carcinoma recurrences with the help of immunoscintigraphy and radioimmunoguided surgery. Clin. Cancer Res., *6:* 363–371, 2000.

18. Profio, A. E., and Balchum, O. J. Fluorescence diagnosis of cancer. Adv. Exp. Med. Biol., *193:* 43–50, 1985.

19. Profio, A. E., Balchum, O. J., and Carstens, F. Digital background subtraction for fluorescence imaging. Med. Phys., *13:* 717–721, 1986.

20. Dougherty, T. J., Gomer, C. J., Henderson, B. W., Jori, G., Kessel, D., Korbelik, M., Moan, J., and Peng, Q. Photodynamic therapy. J. Natl. Cancer Inst., *90:* 889–905, 1998.

21. Folli, S., Westermann, P., Braichotte, D., Pelegrin, A., Wagnieres, G., van den Bergh, H., and Mach, J. P. Antibody-indocyanin conjugates for immunophotodetection of human squamous cell carcinoma in nude mice. Cancer Res., *54:* 2643–2649, 1994.

22. Vogel, C. A., Galmiche, M. C., Westermann, P., Sun, L.-Q., Pelegrin, A., Folli, S., Bischof Delaloye, A., Slosman, D. O., Mach, J. P., and Buchegger, F. Carcinoembryonic antigen expression, antibody localisation and immunophotodetection of human colon cancer liver metastases in nude mice: a model for radioimmunotherapy. Int. J. Cancer, *67:* 294–302, 1996.

23. Birchler, M., Viti, F., Zardi, L., Spiess, B., and Neri, D. Selective targeting and photocoagulation of ocular angiogenesis mediated by a phage-derived human antibody fragment. Nat. Biotechnol., *17:* 984–988, 1999.

24. Welch, A. J., Gardner, C., Richards-Kortum, R., Chan, E., Criswell, G., Pfefer, J., and Warren, S. Propagation of fluorescent light. Lasers Surg. Med., *21:* 166–178, 1997.

25. Ychou, M., Ricard, M., Lumbroso, J., Rougier, P., Mach, J. P., Buchegger, F., Saccavini, J. C., Lasser, P., Elias, D., Eschwege, F., *et al.* Potential contribution of ^{131}I-labelled monoclonal anti-CEA antibodies in the treatment of liver metastases from colorectal carcinomas: pretherapeutic study with dose recovery in resected tissues. Eur. J. Cancer, *29A:* 1105–1111, 1993.

Clinical Cancer Research

Intraoperative Immunophotodetection for Radical Resection of Cancers: Evaluation in an Experimental Model

Marian Gutowski, Magali Carcenac, Didier Pourquier, et al.

Clin Cancer Res 2001;7:1142-1148.